Impact of Geological–Geophysical Data Integration on Coal Tonnage and Stripping Ratio Estimation in an Open Pit Coal Mine

A Case Study from Ogan Komering Ulu, South Sumatra, Indonesia

Wahyu Jayarana
Master Program in Mining Engineering, Faculty of Engineering, Universitas Sriwijaya, Palembang, Indonesia

Eddy Ibrahim
Master Program in Mining Engineering, Faculty of Engineering, Universitas Sriwijaya, Palembang, Indonesia

Budhi Setiawan
Geological Engineering Study Program, Faculty of Engineering, Universitas Sriwijaya, Palembang, Indonesia

Taufik Toha
Master Program in Mining Engineering, Faculty of Engineering, Universitas Sriwijaya, Palembang, Indonesia

Maulana Yusuf
Master Program in Mining Engineering, Faculty of Engineering, Universitas Sriwijaya, Palembang, Indonesia

Rahmat Wahyudi Putra
Master of Environmental Science, Universitas Negeri Padang, Indonesia

Abstract: Open pit coal plans rely on geological models built from widely spaced drill holes, so errors in seam continuity pass directly into tonnage and stripping ratio forecasts. This study quantifies how integrating infill drilling and electrical resistivity tomography (ERT) with existing drill hole data changes the seam model, and the coal tonnage, overburden volume and stripping ratio derived from it, within an unchanged pit boundary. At a reopened pit in Ogan Komering Ulu, South Sumatra, the initial model predicted 34,518.86 t of coal for the first 2.84 ha excavated, whereas truck counts recorded 2,615.6 t. Two infill holes and four Wenner–Schlumberger ERT lines (600 m in total) were interpreted with the existing drill holes, Seams

Correspondents Author:
Eddy Ibrahim, Master Program in Mining Engineering, Universitas Sriwijaya, Indonesia
Email: eddyibrahim@ft.unsri.ac.id

Received October 5, 2026; Revised October 23, 2026; Accepted October 23, 2026; Published November 6, 2026.

X and Y were remodelled, and volumes were recalculated within the same 22.41 ha boundary. The decisive new information was that the southern infill hole did not intersect Seam Y and that the borehole-calibrated coal response (above 5,000 Ωm) was continuous in the west but faded towards the south and southeast. Seam roofs shifted by −11 to +6 m, and the seams were terminated where both data sets indicated their absence. Estimated coal therefore fell by 34.50% (490,346.96 t, from 1,421,125.56 t to 930,778.60 t), overburden rose by 10.11%, and the stripping ratio increased from 2.48 to 4.17 BCM/t. These changes quantify the effect of the revised seam geometry; support for the revised model comes separately, from its agreement with the infill drilling and with what excavation has exposed. Because the ERT inversions have high RMS errors and only two infill holes were available, the revised estimates are provisional, and the early-mining shortfall cannot be attributed to the initial model alone. For open pit planning, the case shows that a low-cost geophysical check tied to drill holes can change the economics of a short-term pit design before most of it is excavated.

Keywords: coal seam continuity, electrical resistivity tomography, infill drilling, stripping ratio, geological model update.

Introduction

Open pit coal mining commits large amounts of capital and equipment to a mine plan long before most of the coal is exposed. Such a plan depends on a geological model that, in most Indonesian coal concessions, is built from drill holes spaced tens to hundreds of metres apart. If the model places a seam in the wrong position, or assumes a seam that is not there, the error shows up later in the pit as missed coal targets, extra waste removal and repeated changes to the short-term schedule. For this reason, several planning studies treat the geological model as something to be revised as new information comes in. A rolling-horizon scheme that updates the model each period produced better schedules than a fixed two-stage formulation (Armstrong et al., 2021). (Lagos et al., 2022) framed the same problem around the fact that only limited drill hole information is available when the first decisions are made, so the schedule has to adapt as blocks are mined. A related line of work uses incoming information from operating mining complexes to adjust production schedules during operation (Kumar & Dimitrakopoulos., 2021). Indonesian coal operations show the practical side of this problem. In one of the country's largest coal producers, the accuracy of the geological model accounted for 36.5% of the discrepancy between planned and mined coal, and the experts consulted in that study named washouts, burned coal and drill spacing wider than 100 m as typical causes (Bakkula et al., 2025). Monthly model recovery in another Indonesian pit ranged from 73% to 121% within a single quarter because the seams thinned in places the model did not anticipate (Alfariji et al., 2025). Short-term evaluations of mine progress in Jambi have likewise recorded

gaps between the planned and the actual position of the pit (Pasaribu et al., 2024), and monthly progress reviews are routinely used to adjust the following month's plan in open cut coal mines (Hakim et al., 2020). Most of these studies describe and measure the deviation. Much less is written about what a mine should do to correct its model once the deviation has been noticed. The usual response is to drill more holes. Geostatistical drill hole spacing analysis is widely used in Indonesia to link spacing to resource confidence. (Heriawan et al., 2020) showed that seam thickness in the Kutai Basin is spatially non-stationary and that the data had to be split into domains before an optimum spacing could be derived. Relative estimation error has been used to set spacing limits for measured, indicated and inferred coal in Jambi (Fahdli & Setiawan., 2022), the same approach has been tested on coal in the South Sumatra Basin (Putra et al., 2022), and relative kriging standard deviation has served as a basis for resource classification (Ramadhan et al., 2021). Once a pit is open, though, drilling is slow and costly, and the ground between holes is still filled in by interpolation. (Cui et al. ,2025) found that interpolation precision drops when sample points are sparsely distributed, and adaptive interpolation schemes have been proposed specifically to cope with sparse borehole data in 3D geological models (Sun et al., 2022). (Lin et al., 2022) reported that seam thickness predicted from boreholes alone had poor precision and improved it by adding seismic attributes, an indication that a second data source with better lateral coverage is worth having. At shallow depth, electrical resistivity tomography (ERT) can play that role at relatively low cost. Coal is often more resistive than the clays and shales around it; vertical soundings in the Benue Trough recorded 778 to 103,000 Ωm for coal against 99 to 898 Ωm for the host shale (Olatunji & Jimoh., 2020). In practice the contrast is often weaker. (Rupesh et al., 2024) noted that thin coal layers are hard to separate from a resistive background without borehole correlation, and (Yang et al., 2024) observed that coal seams in their open pit were only slightly more resistive than porous sandstone. The agreement between ERT and borehole logs is also best where survey lines pass close to the holes (Zakaria et al., 2026). In coal mining, resistivity imaging has been used to locate concealed structures within seams (Guo et al., 2020) and to map old workings with Wenner–Schlumberger and dipole–dipole arrays combined into pseudo-3D models (Bharti et al., 2022). Experience from Indonesian coal pits points the same way. In an East Kalimantan pit, a Wenner–Schlumberger section constrained with lithological, gamma ray and density logs agreed best with the borehole data among the arrays tested, yet the coal seams there had resistivities of only 24 to 34 Ωm (Lepong et al., 2018), far below the values reported from the Benue Trough. The resistivity of coal is therefore site-specific and cannot be assigned without local calibration. The two data sources are complementary. Drill holes logged with gamma ray and density tools give the depth and thickness of coal directly, because coal is clearly separated from the enclosing claystone, siltstone and sandstone on these logs, but only at points (Lubis et al., 2024). ERT gives

continuous lateral coverage along a line, with a resolution that decreases with depth and depends on the electrode array (Dahlin & Zhou., 2004; Loke et al., 2013). Combined, the drill holes anchor the seam picks and the lithological meaning of the resistivity image, while ERT tests whether the seams continue between the holes. This combination suits the study area, where the upper parts of the target seams lie within the investigation depth of a short surface array, the coal is enclosed by clay-rich overburden and sandstone, and the open question concerned the lateral continuity of the seams between holes rather than their detailed thickness. In most of the ERT studies cited above, the work stops once a seam has been mapped or a resource has been estimated. We found few cases in which the correction was carried through to the mine plan itself, meaning the tonnage, overburden volume and stripping ratio of a pit design that was already being mined when production contradicted the model. More specifically, we are not aware of a study that compared coal tonnage, overburden volume and stripping ratio before and after a geological–geophysical model update within the same, fixed pit design boundary, so that the change could be attributed to seam geometry alone. The planning-scale consequence of such an integration, as distinct from its effect on the seam map, therefore remains largely unquantified. Interpretation choices also carry their own uncertainty, which can be treated explicitly in 3D modelling (Madsen et al., 2022). A model correction based on new data is therefore best judged by how much it changes the numbers that planners actually use. The present case comes from the Muara Enim Formation of the South Sumatra Basin, where coal seam character varies between pits (Karyadi & Setiawan., 2023) and seam geometry has been modelled with kriging from drill hole data (Kurniawan., 2021). Mining at the study pit resumed in 2025 after a five-year pause, and in the first months of operation only a small fraction of the predicted coal was found. The objective of this paper is to evaluate how two infill drill holes and four ERT lines, combined with the existing drill hole data, change the geometry and lateral continuity of the mined seams, and how much this revision alters coal tonnage, overburden volume and stripping ratio inside an unchanged 2025 pit boundary. Three questions are addressed: (i) how the borehole-calibrated ERT sections change the interpreted continuity and roof elevation of Seams X and Y; (ii) how much these geometric changes alter coal tonnage, overburden volume and stripping ratio when the pit boundary, topography, block model and coal density are held constant; and (iii) how far the revised figures can be relied upon, given the limitations of the data. The main contribution is not a new integration procedure, since borehole-calibrated ERT is an established technique, nor the revised resource figure itself. It is the demonstration, in an operating pit, of how much geological uncertainty in seam continuity propagates into the planning quantities used for short-term decisions, together with an explicit separation of the results that rest on measured evidence from those that rest on interpretation. We also discuss the consequences for short-term planning and the factors that limit the reliability of the geophysical data.

Research Method

Study area and the observed deviation

The study pit lies in Gunung Kuripan Village, Pengandonan District, Ogan Komering Ulu Regency, South Sumatra, about 43 km from Baturaja. The mining licence covers 1,199 ha, and the annual pit design for 2025 covers 22.41 ha (Figure 1). Mining in the pit stopped in 2020 and resumed in 2025; water has since accumulated in the older excavations on the western and eastern sides. The coal is black to brownish black, moderately hard to hard and sub-bituminous, with thin claystone and sandstone partings that suggest a fluvial–deltaic setting. Three seams are recognised: Seams X and Y are the mining targets in the 2025 design, and Seam Z lies deeper and is outside the 2025 plan.

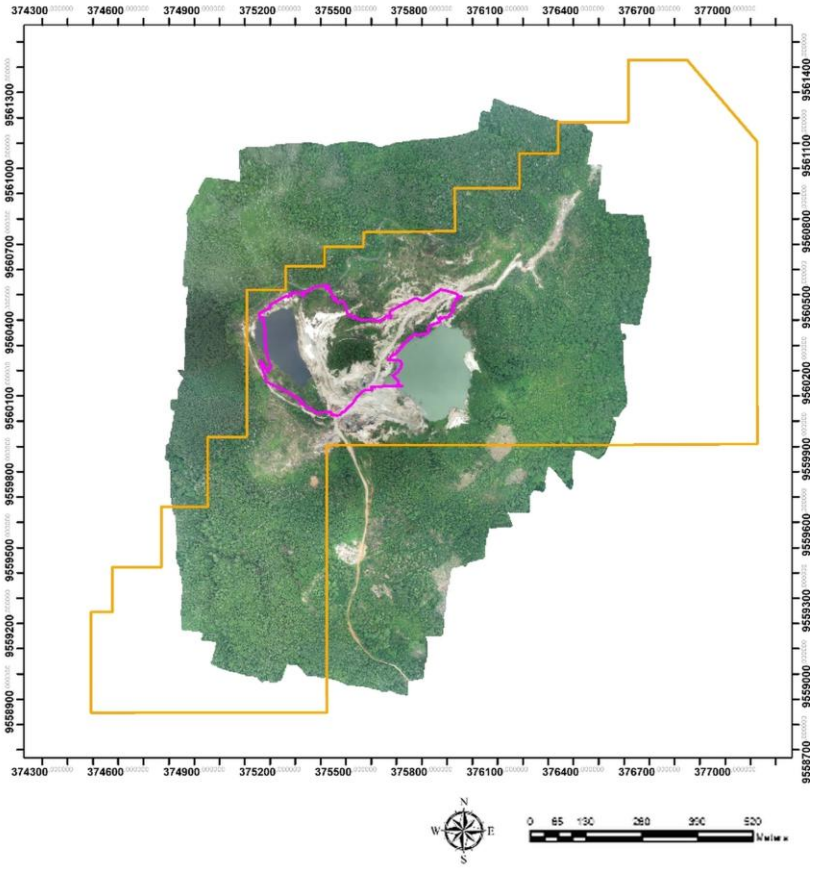


Figure 1 Aerial image of the study area showing the licence boundary (orange) and the 2025 pit design boundary (magenta); coordinates in UTM (m)

By February 2025 the pit had been opened over 2.84 ha, or 12.67% of the planned area. Truck counts over that area recorded 2,615.6 t of coal, whereas the initial model, built in MineScape 5.7 from the existing drill holes, predicted 34,518.86 t for the same ground. Actual recovery was therefore about 7.6% of the modelled tonnage. Both figures refer to the same 2.84 ha opened area and to the same period, from the resumption of mining to the end of February

2025: the predicted figure is the coal tonnage of the initial model for the ground excavated in that area and period, and the recovered figure is the coal hauled from it. Because truck counts are an approximate measure, the comparison is used here only as an indication that the model and the ground disagreed, not as a reconciliation figure; other possible causes of the difference are discussed in the Results. A joint deviation report prepared by the contractor and the licence holder in January 2025 noted that coal predicted at RL +180 in the southern part of the pit was not found during excavation. In the initial model Seam Z had been interpolated as continuous between the existing holes, which made a large coal body appear in the southern pit.

Data

Secondary data consisted of topographic survey data, collar coordinates, lithological and stratigraphic logs of the existing drill holes, the licence and pit boundaries, and the initial geological model. Primary data consisted of two infill holes, BE_2506C and BE_2508C, drilled inside the 2025 pit boundary between existing holes and close to the active mining face, and four ERT lines. The infill holes were cored and logged with gamma ray and density tools, which gave a clear contrast between coal and the enclosing rocks. The new data were acquired as a targeted check of the zone where the model and the mined ground disagreed, while the pit was operating, rather than as a full re-exploration of the pit. The two infill holes were therefore placed where they could test whether the target seams continue southwards from the existing holes, and the ERT lines were used to extend this control laterally between and beyond the holes. The consequences of this limited density of new data for the accuracy and generality of the results are discussed under Limitations.

ERT acquisition

Four lines, A–A′, B–B′, C–C′ and D–D′, were laid out across the zone where the model and the mined ground disagreed (Figure 2). Line A–A′ runs north–south along the western side of the pit across ground that the initial model treated as coal-bearing. Line B–B′ continues A–A′ southwards through the centre of the pit and crosses the existing ramp. Line C–C′ runs west–east in the south of the pit, parallel to the 2025 boundary, and D–D′ crosses diagonally from southwest to northeast over the transition between the pit opening and the natural slope. Each line used 32 stainless steel electrodes at 5 m spacing, giving a line length of about 150 m, a total of 600 m, and an investigation depth of roughly 20 to 35 m. The Wenner–Schlumberger array was chosen for its balance between vertical and lateral sensitivity. Data were recorded with a multichannel resistivity meter and a 32-channel switch box. Contact resistance was kept below 2 kΩ where possible, readings were stacked three to six times, and readings with a standard deviation above 5% were repeated. The coordinates and elevation of every electrode

were surveyed so that topography could be included in the inversion. Apparent resistivity data were inverted in Res2DInv with topography. The quality of each inversion was assessed with the root-mean-square (RMS) error reported by Res2DInv, which expresses the percentage misfit between the measured apparent resistivities and those calculated from the final model (Loke et al., 2013). The RMS values were not used to accept or reject a line outright; instead they determined how much detail of each section was used in the interpretation, as described below and in the Results.

Integration and recalculation

The integration followed four steps. First, coal intervals in the infill holes were placed on the nearest resistivity sections to calibrate the resistivity response of coal against that of the overburden. Second, the lateral persistence of the calibrated high-resistivity response was traced from line to line to test the continuity that the initial model had assumed. Third, the roof and floor surfaces of Seams X and Y were remodelled using the existing holes, the infill holes and the ERT interpretation, with ERT used as a constraint between holes rather than as a substitute for them. Roof elevations of both seams were then compared at seven control points, A to G, along an integrated cross-section. Fourth, overburden volume, coal tonnage per seam and stripping ratio were recalculated for both models using the same topography and the same 22.41 ha boundary, so that any change could be attributed to seam geometry and continuity alone. The stripping ratio was taken as overburden volume in bank cubic metres divided by coal tonnage. Percentage changes were calculated as Change (%) = (V_integrated − V_initial) / V_initial × 100, where V is the coal tonnage, overburden volume or stripping ratio of the respective model. The stripping ratio and its change were calculated from unrounded values (2.4820 and 4.1728 BCM/t), and values in the tables are rounded to two decimals. All elevations are given in metres relative to the mine datum (m RL).

Interpretation criteria and use of ERT in the seam model

Because the resistivity ranges of clay-rich material, sandstone and coal overlap (Table 1), a resistivity value alone was not used to assign a lithology. A zone was interpreted as coal only when four criteria were met: (i) its resistivity was markedly higher than the local background on the same section, with a core above about 4,500–5,000 Ωm; (ii) it formed a laterally continuous, tabular body at an elevation consistent with the seam roof and floor in the nearest drill holes and with the seam dip between them; (iii) it coincided with a logged coal interval where a drill hole lay on or close to the line; and (iv) a comparable response could be followed on more than one line. Zones of about 500 to 1,600 Ωm without coal in a nearby hole were classed as compact non-coal material, mainly sandstone, and zones below about 50 Ωm as clay-rich or water-saturated material. A high-resistivity body that met criteria (i) and (ii) but

could not be checked against a drill hole was treated as inferred, and was not used on its own to add coal to the model. Roof and floor picks of Seams X and Y were taken from the lithological, gamma ray and density logs of every existing and infill hole and were honoured exactly in the revised model. Between holes, the top of the calibrated high-resistivity body was used as a guide to the roof of the upper seam only where criteria (i)–(iv) were met, and the lower seam was positioned using the seam interval observed in the nearest holes. Where the calibrated response was absent on a line and the nearest infill hole did not intersect the seam, the seam was terminated between the last point with coal evidence and the first point without it, instead of being interpolated across the gap as in the initial model. Because of the high RMS errors, ERT was used mainly to decide whether a seam is present or absent between holes; elevations read from ERT were given less weight than drill hole picks and were not used where they conflicted with a drill hole. The revised surfaces were then used with the same block model configuration and coal density as the initial model.

Result and Discussion

Infill drilling

The two infill holes gave different pictures of the seam sequence. In BE_2506C coal was intersected between 23 and 54 m and correlated with Seam Y, with a 2 m parting between 35 and 37 m. BE_2508C, drilled further south in the area where the model had failed, intersected only one main coal interval between 51 and 59 m. This interval was correlated with Seam Z, which is not part of the 2025 mining plan. The absence of a Seam Y interval in BE_2508C was the first direct evidence that the target seams do not continue southwards in the way the initial model had assumed.

Resistivity sections

All four sections show a low-resistivity cover, a moderate middle zone and a resistive lower zone, but the size of the resistive zone differs from line to line. Line A–A′ ranges from about 10 to more than 6,000 Ωm. A low-resistivity layer of 10 to 40 Ωm extends from the surface to about +165 m in the centre of the line and is interpreted as moist or water-saturated material. It is underlain by a moderate zone of 50 to 500 Ωm and, below +165 m, by a high-resistivity body above 500 Ωm whose core exceeds 5,000 Ωm. Line B–B′ shows lower values overall, from 10 to 2,600 Ωm, and the high-resistivity response appears only as a small patch near +145 m, which may represent a thin coal layer or a parting. On C–C′ a low-resistivity cover of about 2 to 65 Ωm is underlain by values above 550 Ωm in a basin-shaped body that is deepest near the centre of the line, between 70 and 90 m along the profile. Line D–D′ grades from 10 to 25 Ωm in the southwest to about 200 Ωm, and values above 5,000 Ωm do not appear

towards the northeast. Table 1 summarises the interpretation adopted after calibration against the drill holes.

Table 1 Resistivity ranges and their interpretation after calibration against drill hole lithology. The ranges are indicative and overlap. Only the coal interpretation is directly confirmed by a drill hole (BE_2506C on line A–A′); the other interpretations are inferred from the resistivity sections and the lithology of nearby holes

Resistivity (Ωm)	Interpretation
1–20	Water-saturated near-surface material; saturated sandstone
50–550	Moderate resistivity of limited extent; mainly associated with clay-rich intervals
500–5,000	Compact, high-resistivity material; mainly associated with sandstone
> 4,500	Very high resistivity; associated with coal where confirmed by drill holes

The ranges in Table 1 overlap, and they should be read as indicators rather than thresholds. Inverted models also carry uncertainty. The final inversions of A–A′ and C–C′ reached RMS errors of 56.8% and 80.9%, which are high for this method. Strong resistivity contrasts close to the surface are known to distort ERT images over mine sites (Bharti et al., 2023), and the pit surface here combines exposed coal, disturbed fill and ponded water within a few metres. Resistivity of mined strata also changes with hydrological conditions between wet and dry seasons (Bharti et al., 2021), and water seepage zones in coal mine settings show up clearly in ERT and self-potential surveys (Kumar et al., 2021). Both effects may have contributed to the misfit. We therefore only used features in the geological model if they agreed with the drill holes and could be followed on more than one line. These misfits mean that the absolute resistivity values and the exact shape of individual bodies are uncertain, particularly near the surface and at the ends of the lines, where data coverage is lowest. In our view they do not invalidate the limited use made of the sections here, for three reasons. First, the interpretation relies on contrasts of about an order of magnitude, between cores above 5,000 Ωm and surroundings of 500–1,600 Ωm or less, which are much larger than the local distortion expected from the misfit. Second, the key observation, that the high-resistivity body is present in the west and absent towards the south and southeast, is repeated on several lines and is not a feature of a single section. Third, it agrees with two independent observations: the absence of Seam Y in BE_2508C and the missing coal at RL +180 reported during excavation. Fine detail, such as small patches or the exact depth of boundaries, was not used. The RMS errors nevertheless remain a source of uncertainty in the position of the inferred seam limit, which is considered further under Limitations.

Correlation between drill holes and resistivity

Figure 3 places the infill holes on the nearest sections. On A–A′, the zone above 5,000 Ωm lies at the same elevation as the upper part of the coal interval logged in BE_2506C, which

supports reading the strongest resistivity response on this line as coal. For BE_2508C on C–C′ the link is weaker. The Seam Z interval in that hole, at 51 to 59 m depth, lies below the investigation depth of the line, so the section cannot image Seam Z itself. It does show, however, that the zone above 5,000 Ωm is confined to the western part of the line and does not extend eastwards to BE_2508C, where values stay mostly between about 500 and 1,600 Ωm. Together with the absence of Seam Y in BE_2508C, this is taken to mark the eastern and southern limit of the Seam Y body rather than a change in seam depth.

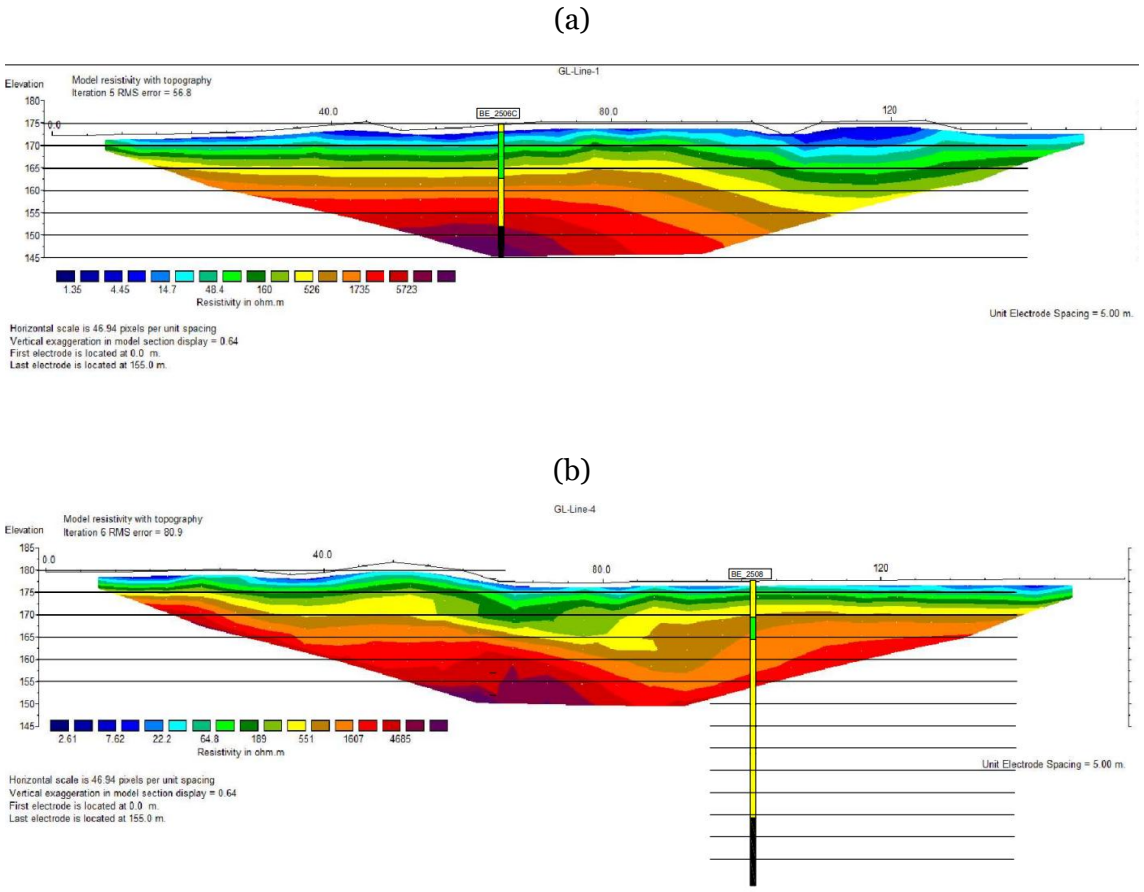


Figure 2 Drill hole correlation with inverted resistivity sections: (a) BE_2506C on line A–A′; (b) BE_2508C on line C–C′. The coal interval in each hole is measured; the extent of the high-resistivity body away from the holes is interpreted from ERT

Taken together, the high-resistivity response is continuous on A–A′, patchy on B–B′ and absent at depth towards the southeast on D–D′. This is the same area where the initial model had connected the existing holes with continuous surfaces. The ERT results indicate that the target seams terminate, or thin below the resolution of the survey, before reaching the southern and southeastern part of the pit. This agrees with the field observation that coal was missing at RL +180. A 3D acquisition with flexible electrode positions, of the kind already used inside coal mines (Pang et al., 2022), would map this limit more completely than four 2D lines can.

Updated seam model

Figure 2 compares the structure contours of the Seam X roof before and after integration. In the initial model the contours strike roughly north–south across the whole pit. In the updated model the strike swings towards west–east in the southern part, and the seam does not continue past the zone outlined by the infill holes and the ERT lines. A change in strike of this kind can result from folding, flexure or faulting. Loss of a seam, however, can equally come from stratigraphic causes such as pinch-out, facies change or washout, and the present data show no clear offset of the seams. The feature is therefore treated as a seam discontinuity associated with a change in bed geometry, and the cause is left open until more drilling is available.

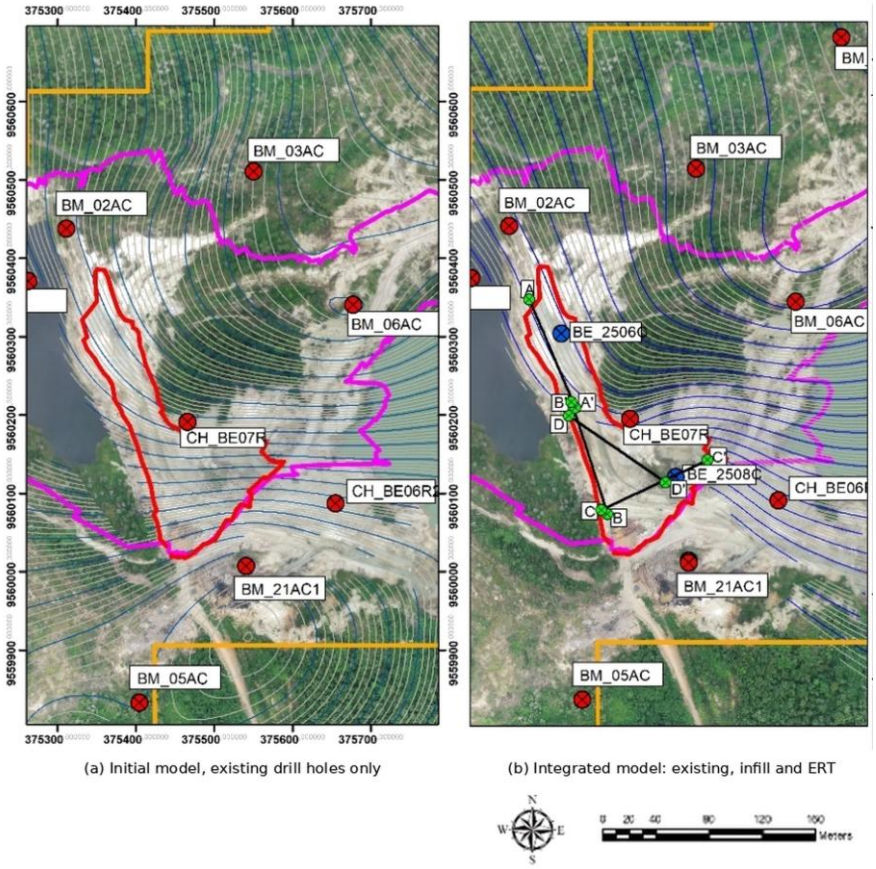


Figure 3 Seam X roof structure contours from (a) the initial model and (b) the integrated model. Red circles: existing drill holes; blue circles: infill holes; green lines: ERT lines; red line: mining progress in February 2025; magenta line: 2025 pit design boundary; orange line: licence boundary. Contours at drill holes are controlled by drill hole picks; the southern termination of the seam in (b) is inferred from the ERT lines and from the absence of Seam Y in BE_2508C

The integrated cross-section in Figure 4 shows how the roofs of Seams X and Y moved after the new data were added. Roof elevations at the seven control points are compared in Table 2. Changes in Seam X range from −9 to +6 m and changes in Seam Y from −11 to +6 m. The largest shift occurs at point E, where the Seam X roof dropped by 9 m and the Seam Y roof by

11 m. Points B, C and F barely moved, which is expected where the existing holes already controlled the surface. The pattern is consistent with corrections concentrated in the parts of the pit that had the least drill hole control. These geometric changes explain the volumetric results reported below. Where the roof was lowered (points A, E and G, by 5 to 11 m), the overburden above the seams thickens, and where the pit floor is fixed by the design, part of the seam can fall below it. Where the roof rose (point D, +6 m), the opposite occurs locally, but this is outweighed by the lowering elsewhere and, above all, by the termination of the seams in the southern and southeastern pit, where coal assumed in the initial model is replaced by waste. Seam termination therefore acts on both terms of the stripping ratio at once: it removes coal from the denominator and adds rock to the numerator.

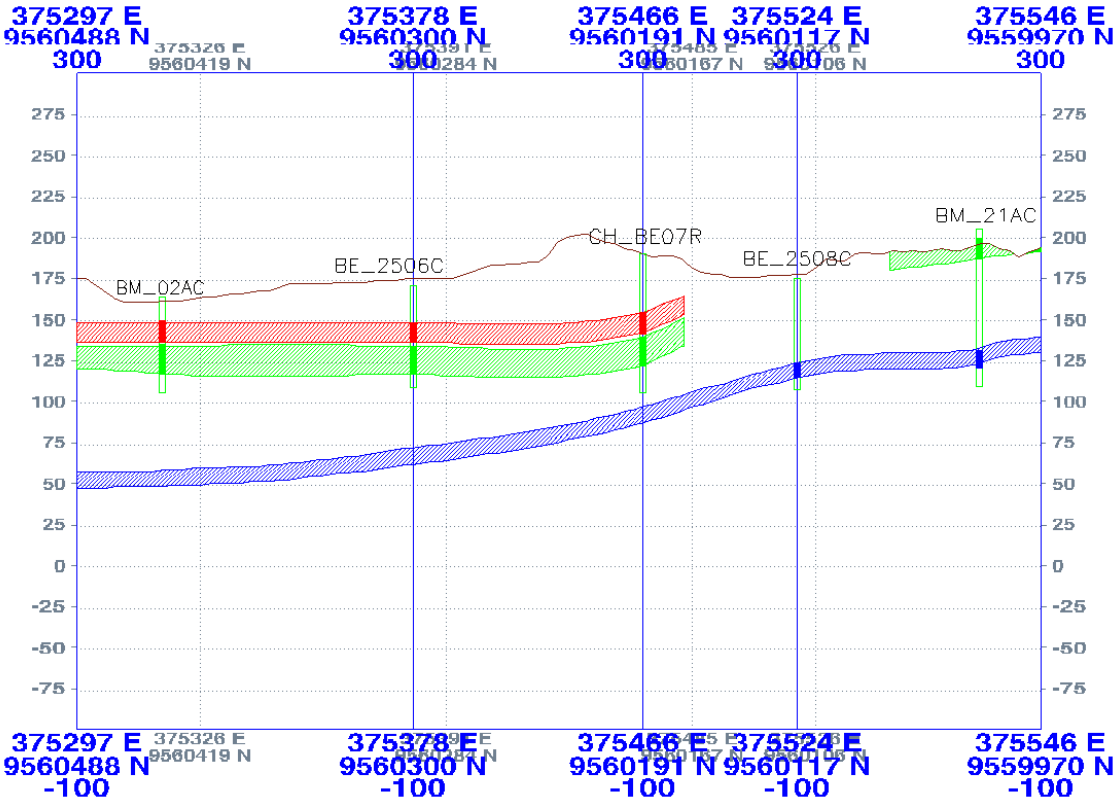


Figure 4 Cross-section through the integrated model showing Seam X (red), Seam Y (green) and Seam Z (blue). Seam positions at drill holes are measured; between holes they are interpolated with ERT as a constraint. Control points A–G of Table 2 lie along this section

Table 2 Roof elevation of Seams X and Y at control points in the initial and integrated models (m RL)

Point	Initial X	Initial Y	Updated X	Updated Y	Change X	Change Y
A	165	151	157	143	−8	−8
B	149	135	149	135	0	0
C	150	137	149	136	−1	−1
D	137	122	143	128	+6	+6
E	121	106	112	95	−9	−11
F	141	125	142	126	+1	+1
G	114	96	106	91	−8	−5

Effect on tonnage, overburden and stripping ratio

Table 3 compares the volumes calculated from the two models within the same 22.41 ha boundary. Because the area and the topography were held constant, the differences reflect seam geometry and continuity only. Coal fell from 1,421,125.56 t to 930,778.60 t, a reduction of 490,346.96 t or 34.50%. The loss is spread across both target seams: Seam X decreased by 37.54% and Seam Y by 32.04%. Overburden increased by 356,753.85 BCM, or 10.11%, because the material that the initial model had counted as coal is now waste. The two changes act in the same direction, so the stripping ratio rose from 2.48 to 4.17 BCM/t, an increase of 68.12%. Percentage changes follow the definition given in the Research Method.

Table 3 Volumes and stripping ratio within the 2025 pit boundary for the initial and integrated models

Parameter	Initial model	Integrated model	Difference	Change (%)
Area (ha)	22.41	22.41	0	0.00
Overburden (BCM)	3,527,207.13	3,883,960.98	+356,753.85	+10.11
Coal, total (t)	1,421,125.56	930,778.60	−490,346.96	−34.50
Seam X (t)	637,207.20	398,024.03	−239,183.17	−37.54
Seam Y (t)	783,918.36	532,754.56	−251,163.79	−32.04
Stripping ratio (BCM/t)	2.48	4.17	+1.69	+68.12

Note: Change (%) = (integrated − initial) / initial × 100. Stripping ratio = overburden (BCM) / coal (t), calculated from unrounded values (2.4820 and 4.1728 BCM/t). Values are rounded to two decimals; the seam tonnages therefore add up to the total within 0.01 t.

For a pit that has only just reopened, the stripping ratio matters more than the tonnage figure on its own. Under the initial model each tonne of coal needed about 2.5 BCM of waste removal; under the integrated model it needs about 4.2 BCM. In practice the excavator and truck fleet would have to move around 68% more waste for every tonne of coal produced. The stripping ratio of a pit also depends on design choices such as slope geometry (Sirnipson et al., 2020), and none of those choices changed here. The increase is entirely geological, and in our view it justifies a review of the pit limit and the mining sequence before the remaining 87% of the design area is opened. In practical terms the revision affects the plan in three ways. First, the coal expected from the 2025 design falls by about one third, so production targets and schedules based on the initial model need to be revised. Second, the higher stripping ratio raises waste haulage per tonne and therefore the fleet hours, fuel and dump capacity required per tonne of coal; if the break-even stripping ratio of the operation lies between 2.48 and 4.17 BCM/t, the economic pit limit itself changes. Third, for resource assessment, coal south and southeast of the inferred seam limit should no longer carry the confidence implied by the initial model and should be reported, if at all, at a lower confidence level until it has been tested by drilling. A practical response is to mine first the western and central part of the pit, where

seam continuity is supported by both drill holes and ERT, and to defer the southern part until additional holes are available. Block model settings and coal density could change the size of the correction, although probably not its direction. Volumetric results from seam models are sensitive to block model settings (Fikri et al., 2024), and tonnage depends on the density assigned to coal, which is itself a recognised source of uncertainty in coal resource work (Roux., 2021). Both models in this study used the same block configuration and the same density, so the comparison is internally consistent. Absolute tonnages, however, should still be treated with caution. The early-mining figures need to be interpreted with care. The predicted 34,518.86 t and the recovered 2,615.6 t refer to the same area and period, but the shortfall of about 92% cannot be attributed to the initial geological model alone. Several operational factors could have contributed: (i) coal that had been exposed but not yet loaded and hauled at the cut-off date would be missing from the truck counts; (ii) truck counts based on nominal payloads are approximate, and coal placed in temporary stockpiles or loaded out with waste would not be recorded as coal; (iii) losses and dilution at the roof, floor and partings reduce recovered tonnage relative to in-situ tonnage; and (iv) the surface used for the prediction may not fully reflect excavation, slumping or weathering of coal near the old pit walls before mining stopped in 2020. These factors can explain part of the difference, but probably not all of it, because the joint deviation report recorded that coal predicted at RL +180 was not found at all, and BE_2508C confirmed the absence of Seam Y in the same area. For this reason the reduction of about one third over the full 22.41 ha, obtained by holding everything except seam geometry constant, is a more meaningful measure of the model correction than the ratio observed in the first 2.84 ha. That the largest corrections occur in the southern part of the pit, where excavation started and where the new data are densest, is consistent with both observations. A formal reconciliation of model, survey and production tonnages as mining advances is needed to separate the geological and operational parts of the discrepancy.

Limitations

This study has several limitations, and they bear directly on how the revised figures should be used. First, only two infill holes were drilled, and only one of them (BE_2508C) lies in the southern area where the seam limit was redrawn, so the position of that limit between holes is constrained mainly by geophysics and has not yet been verified independently. Second, the ERT lines are short and shallow, do not reach Seam Z and cover only part of the pit; the interpretation therefore cannot be extended with confidence to the rest of the design area or to other pits, and the results should be read as a site-specific case. Third, the inversions of A–A′ and C–C′ have high RMS errors, which limit confidence in absolute resistivity values and in the depth of boundaries, and the resistivity ranges of clay-rich material, sandstone and coal

overlap, so the interpretation depends on borehole calibration and on the criteria set out in the Research Method. Fourth, the two models are internally consistent with each other, but neither has yet been reconciled with production over a substantial part of the pit. To make the basis of the results explicit, Table 4 separates measured field evidence, interpreted geological boundaries and calculated estimates. The tonnage, overburden and stripping ratio of the integrated model are calculated quantities that inherit the uncertainty of the interpreted boundaries. They show the direction and approximate size of the correction, not a validated resource figure, and should be treated as provisional.

Table 4 Basis of the main results: measured field evidence, interpreted geological boundaries and calculated estimates

Category	Items in this study	Main source of uncertainty
Measured field evidence	Coal intervals, depths and thicknesses in BE_2506C and BE_2508C (core, gamma ray and density logs); logs of the existing drill holes; apparent resistivity data on four lines; surveyed topography and electrode positions; truck-count coal tonnage for the first 2.84 ha	Drill holes are point data; truck counts are approximate
Interpreted geological boundaries	Lithology assigned to resistivity zones (Table 1); lateral limit of Seams X and Y in the southern and southeastern pit; roof elevations between drill holes (Table 2); cause of the seam loss	Overlapping resistivity ranges; RMS errors of 56.8% (A–A′) and 80.9% (C–C′); one infill hole in the southern area
Calculated estimates	Coal tonnage per seam, overburden volume, stripping ratio and their changes (Table 3)	Inherit the uncertainty of the interpreted boundaries; depend on block model settings and coal density

A repeat survey at a different season would help separate lithology from moisture effects, as time-lapse ERT and self-potential monitoring has done at other coal mining sites (Saurabh et al., 2020). Further drilling at the inferred seam limit would also test the interpretation directly. The integrated model is currently being used as the base case for geostatistical estimation and probabilistic tonnage analysis, which will be reported separately.

Conclusions

This study set out to determine how infill drilling and borehole-calibrated ERT change the seam model of a reopened coal pit, and how far that change carries into the planning quantities. Three findings answer this objective. First, the new data changed the interpreted geometry of the target seams mainly by limiting their lateral extent: the coal response confirmed in BE_2506C is continuous in the west but absent towards the south and southeast, where BE_2508C did not intersect Seam Y, and the roofs of Seams X and Y moved by −11 to +6 m, most where drill hole control had been weakest. Second, with the pit boundary, topography, block model and density held constant, this revision reduced estimated coal by

34.50% (from 1,421,125.56 t to 930,778.60 t), increased overburden by 10.11% and raised the stripping ratio from 2.48 to 4.17 BCM/t. For the mine, this means about one third less coal from the 2025 design and roughly 68% more waste to be moved per tonne of coal, enough to require a review of the pit limit, the mining sequence and the fleet plan before the remaining 87% of the design area is opened. Third, the revised model agrees better with what excavation and the infill drilling have shown, but this agreement is not yet a validation. The southern seam limit rests on one infill hole and on ERT sections with high inversion errors and overlapping resistivity ranges, and the early-mining shortfall may partly reflect operational factors. The integrated estimates should therefore be regarded as a provisional, better-constrained base case rather than a demonstrably more accurate resource, and the integration as a quick and relatively inexpensive screening step rather than a substitute for drilling. Before the revised model is used for longer-term planning or resource reporting, we recommend (i) additional cored and geophysically logged holes across the inferred seam limit in the southern and southeastern pit; (ii) longer ERT lines or a 3D survey with greater investigation depth, repeated in a different season, to reduce and quantify the inversion misfit; and (iii) a regular reconciliation of model, survey and production tonnages as mining advances. The contribution of the study is a field case in which the effect of geological–geophysical integration is traced through to the tonnage, overburden and stripping ratio of an operating pit design, with an explicit distinction between measured, interpreted and calculated results.

Acknowledgements

The authors thank the licence holder and the mining contractor for access to the drill hole, survey and production data used in this study.

References

Alfariji, M., Silviana, S., & Kumoro, A. C. (2025). Evaluasi model batu bara dan sequence tambang PIT X periode triwulan 3 tahun 2024 [Evaluation of the coal model and mining sequence of Pit X for the third quarter of 2024]. *Jurnal Profesi Insinyur Indonesia, 3*(2), 94–101. https://doi.org/10.14710/jpii.2025.26860

Armstrong, M., Lagos, T., Emery, X., Homem-de-Mello, T., Lagos, G., & Sauré, D. (2021). Adaptive open-pit mining planning under geological uncertainty. *Resources Policy, 72*, 102086. https://doi.org/10.1016/j.resourpol.2021.102086

Bakkula, O., Wibisono, D., Basri, M. H., & Siallagan, M. (2025). Towards resilience in the value chain of coal mining upstream: An agent-based modeling and simulation to improve coal discrepancy. *Discover Applied Sciences, 7*(1), 22. https://doi.org/10.1007/s42452-024-06375-2

Bharti, A. K., Prakash, A., Verma, A., Oraon, J., Chaudhary, D. K., Kumar, S., & Singh, K. K. K. (2022). Mapping of decades-old underground coal mine workings using electrical resistivity tomography. *Journal of Earth System Science, 131*(4), 258. https://doi.org/10.1007/s12040-022-02008-7

Bharti, A. K., Prakash, A., Verma, A., & Singh, K. K. K. (2021). Assessment of hydrological condition in strata associated with old mine working during and post-monsoon using electrical resistivity tomography: A case study. *Bulletin of Engineering Geology and the Environment, 80*, 5159–5166. https://doi.org/10.1007/s10064-021-02208-3

Bharti, A. K., Singh, S. K., Pal, S. K., Singh, K. K. K., Prakash, A., Bhattacharjee, R., & Kumar, L. (2023). Electrical resistivity tomography technique coupled with numerical modelling: A case study for stability analysis. *Geophysical Prospecting, 71*(7), 1368–1384. https://doi.org/10.1111/1365-2478.13382

Cui, M., Hou, E., Lu, T., Hou, P., & Feng, D. (2025). Study on spatial interpolation methods for high precision 3D geological modeling of coal mining faces. *Applied Sciences, 15*(6), 2959. https://doi.org/10.3390/app15062959

Dahlin, T., & Zhou, B. (2004). A numerical comparison of 2D resistivity imaging with 10 electrode arrays. *Geophysical Prospecting, 52*(5), 379–398. https://doi.org/10.1111/j.1365-2478.2004.00423.x

Fahdli, M., & Setiawan, B. (2022). Determination of relative error in coal resource classification based on geostatistical drill hole spacing analysis: A case study of coal deposits at Batang Hari, Jambi. *Jurnal Geomine, 10*(2), 145–155.

Fikri, H. N., Nurhakim, N., Fauzi, R., Novianti, Y. S., Santoso, E., & Putri, K. S. (2024). Variasi blok model pada pemodelan seam batu bara [Block model variation in coal seam modelling]. *Jurnal GEOSAPTA, 10*(1), 47–52.

Guo, W., Liu, S., Liu, Y., & Chen, S. (2020). Application of electrical resistivity imaging to detection of hidden geological structures in a single roadway. *Open Geosciences, 12*(1), 1083–1093. https://doi.org/10.1515/geo-2020-0175

Hakim, A., Dwiatmoko, M. U., & Melati, S. (2020). Review kemajuan tambang bulan November 2019 dan perencanaan tambang bulan Desember 2019 di tambang terbuka batubara [Review of November 2019 mine progress and December 2019 mine planning in an open pit coal mine]. *Jurnal Geomine, 8*(3), 181–192.

Heriawan, M. N., Pillayati, P., Widodo, L. E., & Widayat, A. H. (2020). Drill hole spacing optimization of non-stationary data for seam thickness and total sulfur: A case study of coal deposits at Balikpapan Formation, Kutai Basin, East Kalimantan. *International Journal of Coal Geology, 223*, 103466. https://doi.org/10.1016/j.coal.2020.103466

Karyadi, R., & Setiawan, B. (2023). Karakteristik seam batubara berdasarkan analisa proksimat pada Formasi Muara Enim di Pit Middle West PT. Bhumi Sriwijaya Perdana

Coal, Kabupaten Musi Banyuasin, Sumatera Selatan [Coal seam characteristics based on proximate analysis in the Muara Enim Formation, Middle West Pit, PT Bhumi Sriwijaya Perdana Coal, Musi Banyuasin Regency, South Sumatra]. *Ophiolite: Jurnal Geologi Terapan, 5*(2), 52–61. https://doi.org/10.56099/ophi.v5i2.p52-61

Kumar, A., & Dimitrakopoulos, R. (2021). Production scheduling in industrial mining complexes with incoming new information using tree search and deep reinforcement learning. *Applied Soft Computing, 110*, 107644.

Kumar, R., Pal, S. K., & Gupta, P. K. (2021). Water seepage mapping in an underground coal-mine barrier using self-potential and electrical resistivity tomography. *Mine Water and the Environment, 40*, 622–638. https://doi.org/10.1007/s10230-021-00788-w

Kurniawan, P. (2021). Coal geometry modeling and resources estimation in Darmo and surrounding area, Muara Enim, South Sumatra. *Indonesian Journal of Economic Geology, 1*(1), 85–91. https://doi.org/10.51835/ijeg.2021.1.1.344

Lagos, T., Armstrong, M., Homem-de-Mello, T., Lagos, G., & Sauré, D. (2022). A framework for adaptive open-pit mining planning under geological uncertainty. *Optimization and Engineering, 23*, 111–146. https://doi.org/10.1007/s11081-020-09557-0

Lepong, P., Supriyanto, Wahyuningsih, S., & Hardiyanto. (2018). Application of multi-array electrical resistivity tomography in PT. Bukit Baiduri Energi coal mining, East Kalimantan. *Indonesian Mining Journal, 21*(1), 1–7. https://doi.org/10.30556/imj.Vol21.No1.2018.662

Lin, X., Zhang, P., Meng, F., & Liu, C. (2022). A coal seam thickness prediction model based on CPSAC and WOA–LS-SVM: A case study on the ZJ mine in the Huainan coalfield. *Energies, 15*(19), 7324. https://doi.org/10.3390/en15197324

Loke, M. H., Chambers, J. E., Rucker, D. F., Kuras, O., & Wilkinson, P. B. (2013). Recent developments in the direct-current geoelectrical imaging method. *Journal of Applied Geophysics, 95*, 135–156. https://doi.org/10.1016/j.jappgeo.2013.02.017

Lubis, A. M., Larang, M. P., Fahmi, K., & Shah, A. A. (2024). An analysis of coal seam lithology using the well-logging method for correlation of Location X, Musi Banyuasin coalfields, South Sumatra. *Indonesian Journal on Geoscience, 11*(2), 221–229. https://doi.org/10.17014/ijog.11.2.221-229

Madsen, R. B., Høyer, A.-S., Andersen, L. T., Møller, I., & Hansen, T. M. (2022). Geology-driven modeling: A new probabilistic approach for incorporating uncertain geological interpretations in 3D geological modeling. *Engineering Geology, 309*, 106833.

Olatunji, S., & Jimoh, A. T. (2020). Coal exploration using electrical resistivity method in some parts of Benue Trough, Nigeria. *Tanzania Journal of Science, 46*(3), 859–872.

Pang, C., Gao, W., Wu, P., & Wang, L. (2022). Grouting effect detection within the floor of a coal seam using 3D electric resistivity tomography (ERT) with arbitrary electrode positions. *Applied Sciences, 12*(11), 5625. https://doi.org/10.3390/app12115625

Pasaribu, N., Yulanda, Y. A., & Wiratama, J. (2024). Evaluasi kemajuan tambang jangka pendek pada bulan September di Pit Rencana 2023, PT Bukit Tambi, Kab. Batanghari, Provinsi Jambi [Short-term mine progress evaluation for September in the 2023 planned pit, PT Bukit Tambi, Batanghari Regency, Jambi Province]. *JTK (Jurnal Teknik Kebumian), 11*(2), 49–60.

Putra, J. A., Heriawan, M. N., & Widayat, A. H. (2022). *Geostatistical drill hole spacing analysis for coal resource evaluation in the South Sumatra Basin, Indonesia* [Conference paper]. International Symposium on Earth Science and Technology, Fukuoka, Japan.

Ramadhan, M. D., Marwanza, I., Nas, C., Azizi, M. A., Dahani, W., & Kurniawati, R. (2021). Drill holes spacing analysis for estimation and classification of coal resources based on variogram and kriging. *IOP Conference Series: Earth and Environmental Science, 819*, 012026. https://doi.org/10.1088/1755-1315/819/1/012026

Roux, L. (2021). Density—A contentious issue in the evaluation and determination of resources and reserves in coal deposits. *Journal of the Southern African Institute of Mining and Metallurgy, 121*(5), 227–250. https://doi.org/10.17159/2411-9717/17386/2021

Rupesh, R., Tiwari, P., & Sharma, S. P. (2024). Estimation of geotechnical parameters for coal exploration from quasi-3D electrical resistivity measurements. *Minerals, 14*(1), 102. https://doi.org/10.3390/min14010102

Saurabh, Pal, S. K., & Kumar, R. (2020). A time-lapse study using self-potential and electrical resistivity tomography methods for mapping of old mine working across railway tracks in a part of Raniganj coalfield, India. *Environmental Earth Sciences, 79*, 332. https://doi.org/10.1007/s12665-020-09067-3

Sirnipson, L. R., Triantoro, A., & Melati, S. (2020). Analisis korelasi stripping ratio dan overburden ratio berdasarkan kemiringan lereng tunggal pada perancangan tambang batubara [Correlation analysis of stripping ratio and overburden ratio based on single slope angle in coal mine design]. *Jurnal Himasapta, 5*(2), 53–56.

Sun, L., Wei, Y., Cai, H., Xiao, J., Yan, J., & Wu, S. (2022). Adaptive interpolation method for generalized triangular prism (GTP) geological model based on the geometric smoothness rule. *Frontiers in Earth Science, 10*, 808219. https://doi.org/10.3389/feart.2022.808219

Yang, Y., Zhao, C., Di, Y., & Li, Q. (2024). Geological exploration of coal mine burnt rock and waterlogged area boundary based on transient electromagnetic and high-density

electrical resistivity. *Scientific Reports, 14*, 5105. https://doi.org/10.1038/s41598-024-55496-6

Zakaria, M. N., Obiya, H., Azhar, A. T. S., Hidayat, Z. M. N., Aziman, M., Amir, J., & Fakhrurrazi, I. M. (2026). The correlation between electrical resistivity tomography and borehole data at a coastal semi-developed area. *International Journal of Integrated Engineering, 18*(3), 243–256.